Stimulated emission and emission efficiency enhancement in nanopatterned silicon

Efraim Rotem[a], Jeffrey M. Shainline[b], and Jimmy M. Xu[a,b]

[a]Division of Engineering, Brown University, 184 Hope St., Providence, RI 02912, USA;
[b]Department of Physics, Brown University, 184 Hope St., Providence, RI 02912, USA;

ABSTRACT

1.278μm laser emission has been observed in a SOI structure which has been nanopatterned to contain an array of nanopores. The optical transition is identified to be associated with phononless recombination mediated by the bistable, carbon-related G center. The present work is focused on increasing the luminescence intensity from nanopatterned Si by increasing the number of G centers present in the material. The G center density is increased by increasing the concentration of substitutional atoms in the lattice prior to nanopatterning. To this end, solid-phase epitaxial regrowth of carbon-rich silicon is utilized in order to take advantage of the increased solid solubility of carbon in silicon at the interface between crystalline and amorphous solid silicon.

Keywords:

1. INTRODUCTION

Silicon photonics is an important, rapidly-expanding field of technology that aims to enable the fabrication and integration of optical components with existing CMOS technology.[1–4] Various silicon photonic devices such as waveguides, modulators, and detectors have been successfully demonstrated.[5–8] Active silicon photonic devices such as efficient silicon light emitters and lasers are especially challenging due to the indirect band gap of silicon. Various approaches to overcome this limitation have been investigated. Among these are erbium-doped devices,[9–11] the all-silicon Raman-conversion laser,[12–14] quantum confined structures such as silicon nanocrystals,[15] dislocation-engineered devices[16,17] and hybrid technology for wafer-scale integration of silicon waveguides and InP (or InAlGaAs)-based lasers.[18] Still, the creation of an all-silicon electrically-driven laser has not yet been achieved.

Recently, stimulated emission and optical gain, characteristics of lasing, at 1.28μ m have been observed in periodic nanopatterned crystalline silicon under optical excitation at cryogenic temperatures.[19] The source of this emission is attributed to the bi-stable carbon-substitutional carbon-interstitial (CsCi) complex known as the G center. The emissive G centers were found as early as the 1960's in irradiated silicon.[?] Early studies were interested in investigating the effects of radiation damage via electron, ion or gamma ray bombardment, mostly for the purposes of assessing, containing, and suppressing the undesirable consequences in electronic applications.[20,21] These bombardment techniques necessarily inflict damage on the entire lattice and thereby increase both the electronic and optical losses. Previously, electroluminescence from G centers was demonstrated in an electron-irradiated p-n junction.[22]

2. FABRICATION

2.1. Carbon–enriched silicon using solid phase epitaxial regrowth

Carbon doping of silicon using conventional ion implantation is limited by the low solid solubility of carbon in silicon (on the order of 10^{17} atoms/cm^3). Carbon ion implantation at levels exceeding the solid solubility results in precipitation of SiC. Instead, solid phase epitaxial (SPE) regrowth is employed. This method takes advantage of the increased carbon solubility at the interface between crystalline and amorphous silicon.[23] The silicon crystal is 'pre–amorphized' by Si^+ ion implantation prior to the C^+ ion implantation. If the carbon ion

Further author information: (Send correspondence to J.M.S.)
J.M.S.: E-mail: jeffrey_shainline@brown.edu, Telephone: (401) 863-3010

Table 1. Parameters for implantations utilized for C–enriched Si fabrication. The RTA was performed in an N_2 ambient in the temperature range between 650–900℃ for 10s. The best results were obtained for RTA performed at 800℃.

Step	Species	Dose	Energy	Temperature	Mean Implant Depth	End of range Depth
Amorphization	Si	10^{15}	65keV	-120℃	95nm	200nm
Implantation	C	10^{14}	18keV	24℃	60nm	120nm

Table 2. Nanopore etching recipe.

Temperature	Pressure	Power	Cl_2	BCl_3	Etching time
24℃	50mTorr	100W	20sccm	5sccm	3×2min

dosage is large enough by itself to amorphize the silicon, pre–amorphization is not required. The crystal is then annealed in nitrogen or argon atmosphere to induce SPE re–growth. Substitutional carbon concentrations of up to $7 \times 10^{20}/\mathrm{cm}^3$ were achieved using this method.[24] As re-growth progresses, the interface between crystalline and amorphous silicon moves; it is at this interface that carbon atoms are incorporated into the lattice in substitutional sites. In this work, p–type SOI (250nm Si on 3mm BOX, 20 Ωcm, commercially available from Soitech) was used. The details of the C–enriched Si fabrication are given in table 1.

The concentration of the implanted carbon atoms was approximately $10^{19}/\mathrm{cm}^3$, 400 times more than the manufacturer-specified carbon content of $2.5 \times 10^{16}/\mathrm{cm}^3$. However, the concentration of carbon atoms that occupy substitutional sites after re–crystalization can be much lower. Substitutional carbon in silicon is usually detected by its local vibrational mode IR absorption at $607\mathrm{cm}^{-1}$.[21] In this study, the maximal absorbance at $607\mathrm{cm}^{-1}$—expected if all implanted carbon atoms were incorporated into substitutional sites—was less than 0.1%. This low absorbance was due to the fact that only a thin layer of carbon–rich silicon was present in the samples, making the detection of this absorbance line below the sensitivity limit of available FTIR instrumentation. Therefore, we could not meaningfully and quantitatively evaluate the fraction of C that was actually incorporated as C_s.

2.2. Nanopatterning using AAO

The periodically nanopatterned C–enriched Si structure shown in fig.1c was fabricated using the highly–uniform self–organized AAO nanopore membrane as an etch mask.[19,25] The free-standing AAO membrane was lifted from an aqueous solution by a C–enriched Si wafer and subsequently etched in an RIE machine. The etch recipe used is given in table 2. The fabrication process and an SEM micrograph of the patterned C–enriched Si are shown in fig. 1.

3. NATURE OF THE G CENTER

G centers are known to be formed after bombardment of the silicon lattice by gamma rays, electrons, neutrons or ions. In the present study they are believed to have been formed during the RIE procedure executed to obtain the pores. A schematic of a G center is shown in fig. 2.

While much about the optical properties of G centers has been known for some time,[20] the effects of the nanopatterning may be elemental to the ability of the nanopatterned silicon to achieve lasing action. It is hypothesized that the key physical elements of the nanopatterned silicon structure mentioned above increase electronic population of the G centers embedded in the surfaces of the pores, while minimizing the overall damage to the crystal and thereby keeping the total optical loss of the patterned sample at a minimum.

4. EXPERIMENTAL RESULTS

Fig. 3 shows the photoluminescence spectra at 25K of the nanopatterned C–enriched Si on SOI and of similarly nanopatterned SOI without carbon enrichment. The 514nm line of an argon ion laser was used for excitation. The excitation power was 200mW and the beam spot size was 3mm in diameter. The emitted photoluminescence

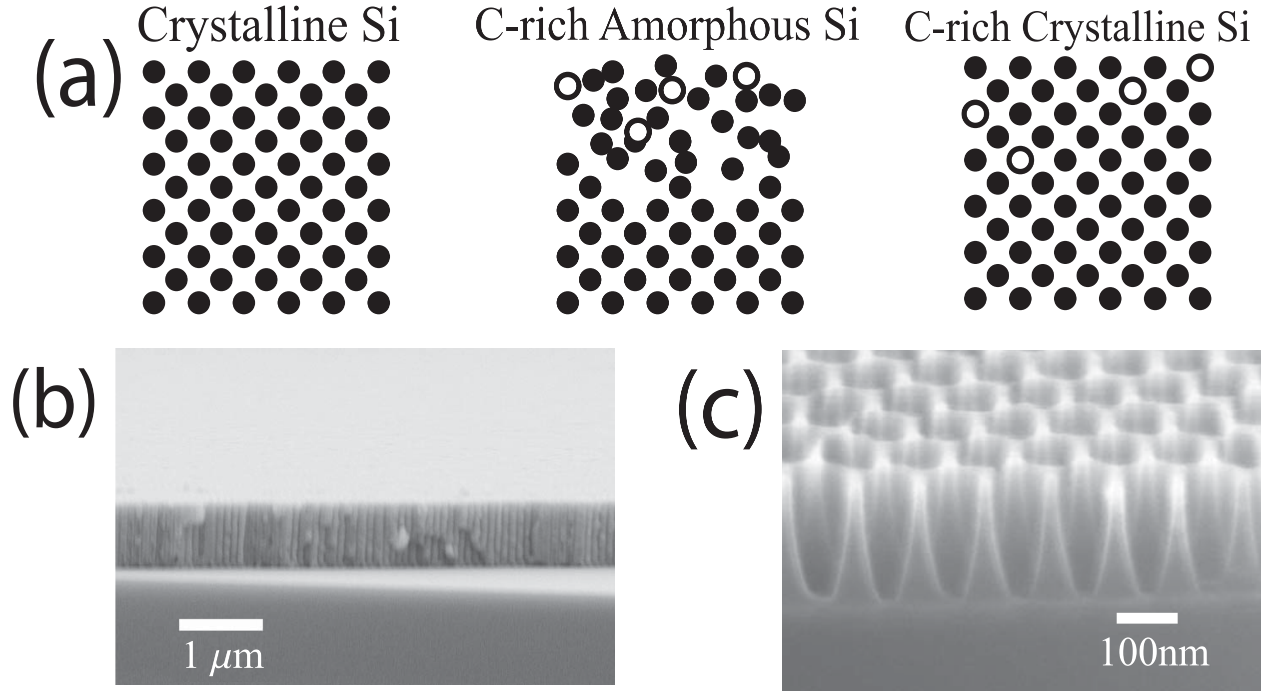

Figure 1. Schematic of the fabrication process. A pristine Si lattice is amorphized by bombarding with Si ions and is then implanted with C ions. The crystal is subsequently re-grown by annealing using the undamaged bottom layer as a seed layer. b. SEM image of an AAO membrane atop a SOI wafer. c. SEM image of an array of nanopores in the SOI wafer resulting from RIE through the AAO etch mask. In this image the AAO has been removed.

was collected using a 3", F/4 concave mirror and focused onto a spectrometer. The resolution of the spectrometer was calibrated using a narrow-line (200kHz) external cavity semiconductor laser and was determined to be 0.13 ± 0.02nm. A cooled InGaAs photodiode array was used to measure the intensity of the PL. The phonon–assisted band–edge PL at 1130nm is similar for both samples and serves as a good reference for comparing the two sets of data. The similarity in the band–edge emission linewidth and peak height is indicative of crystallinity being recovered after the SPE. In the reference nanopatterned SOI sample the G line intensity is 1300 counts per second while in the C–enriched sample the G line intensity is 43,000 counts per second, an increase by a factor of 33. While the results in fig. 3 display the most intense G line observed, G line intensities exceeding 20,000CPS were consistently obtained. The wide band extending from the G line to longer wavelengths consists of several phonon replica modes of the G line.[26] The G line linewidth in the nanopattered SOI reference sample which did not undergo the carbon-enrichment procedure performed was measured to be 1.1 ± 0.1nm at 25K, and the *G* line linewidth in the C–enriched SOI was measured to be 1.5 ± 0.1nm at 25K.

These results confirm that the carbon in the silicon crystal is responsible for the creation of G centers and also provides a path for increasing the efficiency and gain of this material.

5. DISCUSSION

6. DISCUSSION : G CENTER LUMINESCENCE MODEL IN NANOPATTERNED SILICON AND TEMPERATURE DEPENDENCE OF G CENTER LUMINESCENCE

The mechanism of luminescence in p–type material is presented in fig. 4. The G center is bi–stable and can alternate between two atomic configurations referred to as the "A" configuration and the "B" configuration.[20] Both configurations can trap an electron from the conduction band in an "acceptor state" or trap a hole from the

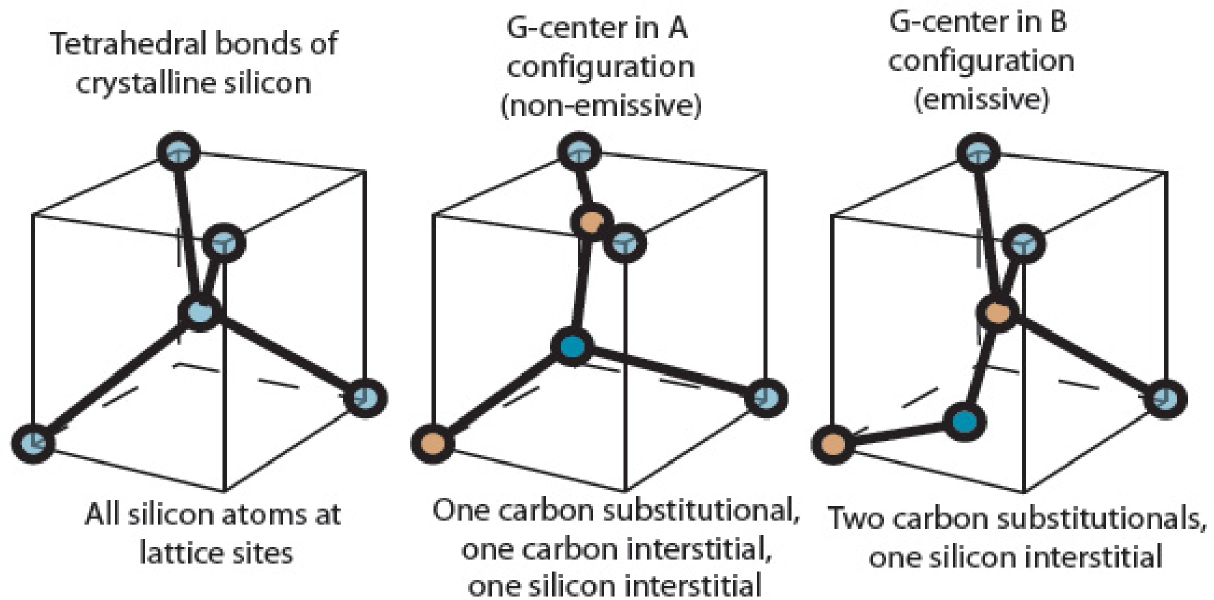

Figure 2. Schematic of the bistable *G*-center. In the non-emissive configuration one silicon and one carbon share the center lattice site. In the emissive B configuration a carbon atom occupies the lattice site and a silicon atom becomes an interstitial.

valence band in a "donor state". Only the *B* configuration, however, is optically active.[20] The process leading to 1.28μm emission is as follows (see fig. 4).

1) In the neutral ground state, the G centers in the system are primarily in the B configuration.

2) In a p–type sample, because the donor state is above the Fermi level, the G center will trap a free hole or the hole of a free exciton and become positively charged. Under no external excitation, the G center will transform to the A^+ configuration, however under optical excitation and below 50K, it remains in the B^+ configuration.

3) The G center will then trap an electron from the conduction band to be in the excited state B^*. The electron and hole appear as clouds in the $E-k$ diagram because their wavefunctions contain contributions from across the Brillouin zone.

4) Phononless emission of a 0.97eV photon occurs; the G center relaxes to the ground state B^0.

There are several important processes limiting the optical activity of point defects in semiconductors.[21] One is that the centers can emit captured electrons (holes) back to the conduction (valence) band. Another is that as temperatures increase, excitons have an exponentially–increased probability of thermally dissociating before they are trapped by an optically active center. In the specific case of the G center there is the additional factor that the center can convert from the optically–active B configuration to the optically–inactive *A* configuration. As the temperature increases, these processes become more efficient, and the luminescence decreases and finally vanishes near 80K.

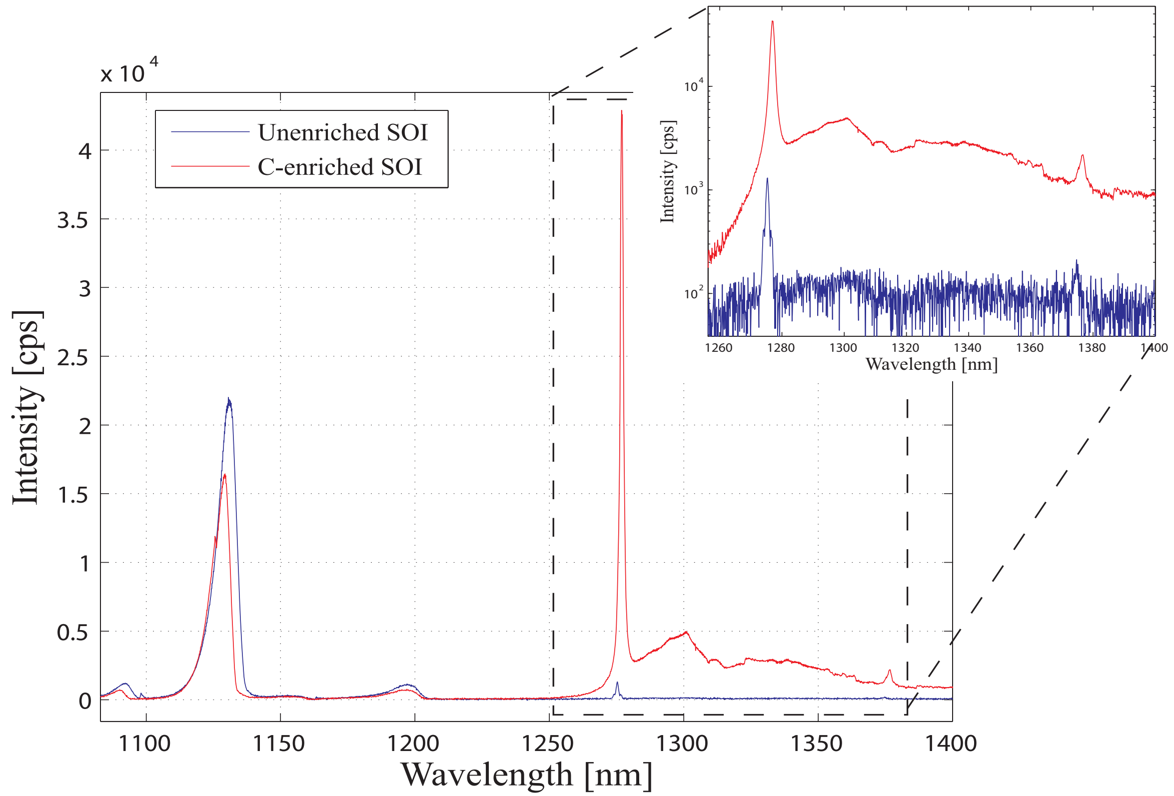

Figure 3. Photoluminescence spectrum of nanopatterned Si and nanopatterned C–enriched Si. The inset shows a semi-log plot of the region containing the G line and phonon replicas.

The marked increase in the G line at cryogenic temperatures in this study is undoubtedly due to an increase in the concentration of C_s in the lattice prior to the etching of pores. We hypothesize that the nanopatterned system is intrinsically beneficial for efficient optical activity; utilizing the nanopatterning technique to create G centers allows for a large surface area with which the energetic ion etchants can interact with the crystal to create silicon self–interstitials which lead to G centers while maintaining the crystallinity, band structure and carrier lifetime of the crystal away from the etched surfaces of the pores. In this way, the unetched regions of the crystal would be able to act under pumping as a carrier reservoir to the G centers embedded in the pore walls. This is made possible by the short distances between the pores (of the order of 10nm) compared with the diffusion lengths of carriers in Si (of the order of microns to hundreds of microns[21]).

The measured linewidths of 1.5nm (C–enriched) and 1.1nm (unenriched) are considerably broader than the reported linewidth of 0.1–0.2nm at 25K.[21,27] This linewidth broadening is likely due to the variety of strain environments[21] experienced by G centers located in the pore walls. TEM images showing evidence of compressive strain in the pore walls are presented in ref. 28. The linewidth broadening in the C–enriched nanopatterned SOI versus the reference nanopatterned SOI is likely due to the presence of a variety of strain environments caused by C_is, C_ss and other residual damage present after amorphization, C implantation, and SPE regrowth. In addition to leading to linewidth broadening, the presence of compressive strain in the pore walls would decrease the band gap locally, which may lead to funneling of excitons from the pristine bulk crystal to the regions dense with G centers near pore walls,[29] facilitating efficient filling of G centers.

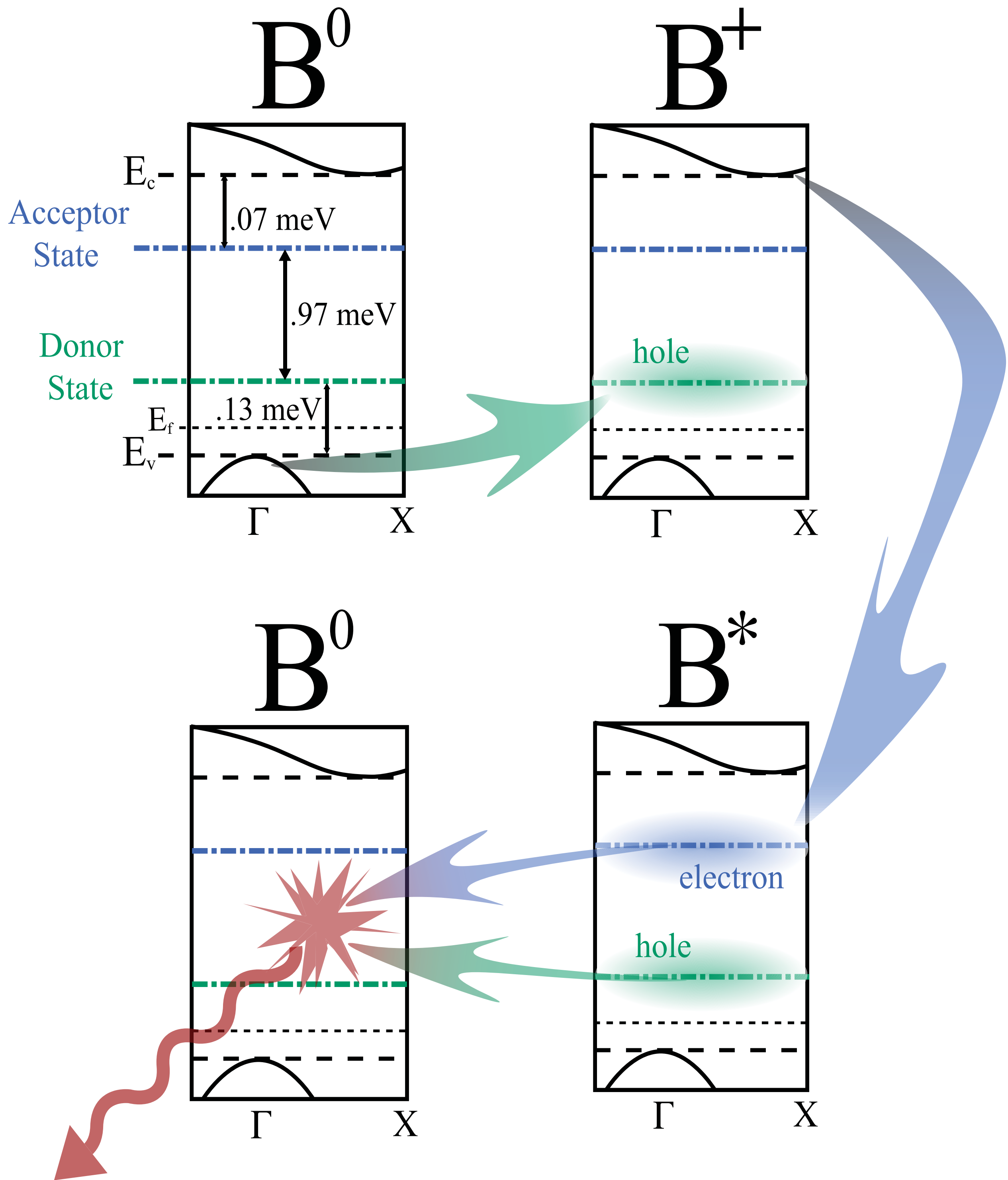

Figure 4. Luminescence mechanism of the G center in p–type silicon.

6.1. Temperature Dependence

The temperature dependence of luminescence from G centers has been documented,[30] and it has been shown that the luminescence from G centers takes a marked decrease at 50K and is entirely extinguished by 100K. This agrees well with the observed temperature dependence of the nanopatterned silicon laser which achieved a maximum operating temperature of 80K.[19] This physical limitation, dictated by the capture kinetics of the G centers versus non-radiative recombination pathways, stands as a formidable barrier to room-temperature operation. However, elements of the existing functionality may offer insight into how the operating temperature may be raised.

The temperature dependence of the G line emission at temperatures above 40K can be modeled according to[27, 30, 31]

$$I_G(T) = I_0 \left[1 + C\mathrm{e}^{-E_a/kT}\right]^{-1}, \tag{1}$$

where I_0 is the intensity at 40K. Eq. 1 models a two level system where the excited state of the G center is thermally depopulated into a higher level separated by E_a, and C is the ratio of degeneracy between these two levels. Previously obtained values for E_a and C are 55 ± 3meV and $2 - 8 \times 10^4$, respectively,[31] 35 ± 5meV (C not given),[27] 68 ± 6mev and 8.9×10^6.[30] The G line intensity of the two samples presented in fig 3 was measured at temperatures between 40K and 80K and fitted according to eq. 1. The obtained values were $E_a = 39$meV, $C = 8300$ for carbon enriched Si and $E_a = 40.1$meV, $C = 3500$ for non-enriched Si. The two values of E_a we obtained are very close and in within the range of previously obtained values. The relatively small values of C are not yet understood, however, the large variations of this constant in previous reports imply that it is very much affected by the measurement setup employed.

The discussed silicon nanostructure is one example of utilizing physical elements such as strain and breaking of k-selection rules to increase optical activity of interstitial complexes embedded in the silicon medium. Nanopatterned SOI fortuitously combines these elements in such a way as to allow for laser action at 1.278 μm at T<80K. Future research must be focused on analyzing each of the physical elements of the model separately to discover how to maximize the contribution of each to laser action. In particular, exploring new ways to locally introduce strain will be crucial to increasing the operating temperature of such point defect silicon lasers because the ability of strained regions to trap excitions, even at high temperatures, is a promising technique to aid in the population of optically active point defects at higher temperatures.

6.2. Conclusions

In conclusion, we have demonstrated that nanopatterning of carbon–rich silicon created via solid–phase epitaxial regrowth after amorphization and carbon implantation can lead to a significant increase in the intensity of the G line emission. An increase by a factor of 33 was achieved in our studies, and samples with intense G line were consistently manufactured. A model has been proposed which describes the capture processes of electrons and holes by G centers which leads to emission of 0.97eV photons from G centers in the B configuration.

Acknowledgement: This work is made possible by support from ONR and DARPA.

REFERENCES

1. G. T. Reed and A. P. Knights, *Silicon Photonics: An Introduction*, Wiley, 2004.
2. L. Pavesi and D. Lockwood, *Silicon Photonics*, vol. 94 of *Topics in Applied Physics*, Springer-Verlag, 2004.
3. B. Jalali and S. Fathpour, "Silicon photonics," *Journal of Lightwave Technology* **24**, p. 4600, 2006.
4. M. Lipson, "Guiding, modulating, and emitting light on silicon—challenges and opportunities," *Journal of Lightwave Technology* **23**, pp. 4222–4238, 2005.
5. A. Liu, R. Jones, L. Liao, D. Samara-Rubio, D. Rubin, O. Cohen, R. Nicolaescu, and M. Paniccia, "A high-speed silicon optical modulator based on a metal-oxide-semiconductor capacitor," *Nature* **427**, pp. 615–618, 2004.

6. L. Liao, D. Samara-Rubio, M. Morse, A. Liu, D. Hodge, D. Rubin, U. D. Keil, , and T. Franck, "High-speed silicon mach-zehnder modulator," *Optics Express* **13**, pp. 3129–3135, 2005.
7. L. Naval, B. Jalali, L. Gomelsky, and J. M. Liu, "Optimization of Si1-xGex/Si waveguide photodetectors operating at lambda= 1.3um," *Journal of Lightwave Technology* **14**, pp. 787–797, 1996.
8. L. Colace, G. Masini, and G. Assanto, "Ge-on-Si approach to the detection of near-infrared light," *IEEE Journal of Quantum Electronics* **35**, pp. 1843–1852, 1999.
9. A. Kenyon, "Erbium in silicon," *Semiconductor Science and Technology* **20**, pp. R65–R84, 2005.
10. M. E. Castagna, S. Coffa, M. Monaco, L. Caristia, A. Messina, R. Mangano, and C.Bongiorno, "Si-based materials and devices for light emission in silicon," *Physica E* **16**, pp. 547–553, 2003.
11. A. Irrera et al., "Light emitting devices based on silicon nanostructures," *Physica E* , 2007. doi:10.1016/j.physe.2006.12.019.
12. O. Boyraz and B. Jalali, "Demonstration of a silicon raman laser," *Optics Express* **12**, p. 5269, 2005.
13. H. S. Rong, Y. H. Kuo, S. B. Xu, A. S. Liu, R. Jones, , and M. Paniccia, "A continuous-wave raman silicon laser," *Nature* **433**, pp. 725–728, 2005.
14. H. S. Rong, Y. H. Kuo, S. B. Xu, A. S. Liu, R. Jones, , and M. Paniccia, "Monolithic integrated raman silicon laser," *Optics Express* **14**, pp. 6705–6712, 2006.
15. L. Pavesi, L. D. Negro, C. Mazzoleni, G. Franzo, and F. Priolo, "Optical gain in silicon nanocrystals," *Nature* **408**, pp. 440–444, 2000.
16. W. L. Ng, M. A. Lourenco, R. M. Gwilliam, S. Ledain, G. Shao, and K. P. Homewood, "An efficient room-temperature silicon-based light-emitting diode," *Nature* **410**, pp. 192–194, 2001.
17. A. V. Yukhnevich, "Towards a silicon laser based on emissive structural defects," *Solid-State Electronics* **51**, p. 489492, 2007.
18. A. W. Fang, H. Park, O. Cohen, R. Jones, M. J. Paniccia, and J. E. Bowers, "Electrically pumped hybrid AlGaInAs-silicon evanescent laser," *Optics Express* **14**, p. 9203, 2006.
19. S. Cloutier, P. Kossyrev, and J. Xu, "Optical gain and stimulated emission in periodic nanopatterned crystalline silicon," *Nature Materials* **4**, p. 887, 2005.
20. L. Song, X. Zhan, B. Benson, and G. Watkins, "Bistable interstitial–carbon–substitutional–carbon pair in silicon," *Physical Review B* **42**, p. 5765, 1990.
21. G. Davies, "The optical properties of luminescence centres in silicon," *Physics Reports* **176**, pp. 83–188, 1989.
22. L. Canham, K. Barraclough, and D. Robbins, "1.3 um light-emitting diode from silicon electron irradiated at its damage threshold," *Applied physics letters* **51**, pp. 1509–1511, 1987.
23. S. Campisano, G. Foti, P. Baeri, M. G. Grimaldi, and E. Rimini, "Solute trapping by moving interface in ion–implanted silicon," *Applied Physics Letters* **37**, pp. 719–722, 1980.
24. J. W. Strane, S. R. Lee, H. J. Stein, S. T. Picraux, J. K. Watanabe, and J. W. Mayer, "Carbon incorporation into Si at high concentrations by ion implantation and solid phase epitaxy," *Journal of Applied Physics* **79**, pp. 637–645, 1996.
25. J. Liang, H. Chik, A. Yin, and J. Xu, "Two–dimensional lateral superlattices of nanostructures: Nonlithographic formation by anodic membrane template," *Journal of Applied Physics* **91**, p. 2544, 2002.
26. G. Davies, E. Lightowlers, and M. do Carmo, "Carbon-related vibronic bands in electron-irradiated silicon," *Journal of Physics C: Solid State Physics* **16**, pp. 5503–5515, 1983.
27. K. Thonke, H. Klemisch, J. Weber, and R. Sauer, "New model of the irradiation-induced 0.97-eV (G) line in silicon: A Cs-Si* complex," *Physical Review B* **24**, pp. 5874–5886, 1981.
28. S. Cloutier, C. Hsu, P. Kossyrev, and J. Xu, "Enhancement of radiative recombination in silicon via phonon localization and selection-rule breaking," *Advanced Materials* **18**, pp. 841–844, 2006.
29. R. Markiewicz, J. Wolfe, and C. Jeffries, "Strain-confined electron-hole liquid in germanium," *Physical Review B* **15**, pp. 1988–2016, 1977.
30. G. Davies, H. Brian, E. Lightowlers, K. Barraclough, and M. Thomaz, "The temperature dependence of the 969 meV 'G' optical transition in silicon," *Semiconductor Science and Technology* **4**, pp. 200–206, 1989.
31. C. E. Jones, E. S. Johnson, W. D. Compton, J. R. Noonan, and B. G. Streetman, "Temperature, stress, and annealing effects on the luminescence from electron-irradiated silicon," *Journal of Applied Physics* **44**, pp. 5402–5410, 1973.